
In Vivo Imaging of Functional Targeting of miR-221 in Papillary Thyroid Carcinoma

Hyun Joo Kim^{1,2}, Young Ha Kim^{1,2}, Dong Soo Lee¹, June-Key Chung^{1,2}, and Soonhag Kim^{1,3}

¹Department of Nuclear Medicine, Seoul National University College of Medicine, Seoul, Korea; ²Laboratory of Molecular Imaging and Therapy of Cancer Research Institute, Seoul National University College of Medicine, Seoul, Korea; and ³Medical Research Center, Seoul National University College of Medicine, Seoul, Korea

MicroRNAs (miRNAs) are small, noncoding RNA molecules that control expression of target genes. The abnormally expressed miRNAs function as oncogenes or tumor suppressors in human cancer. To evaluate the abundant gene regulation of miR-221 in papillary thyroid carcinoma (PTC), we performed microarray analysis and developed a *Gaussia* luciferase (Gluc) reporter system regulated by miR-221. **Methods:** Total RNAs were isolated from pre-miR-221-treated normal human thyroid cells (HT-ori3) and anti-miR-221-treated papillary thyroid cells (NPA). Microarray analysis was performed with 44,000 probes. The messenger RNA levels of target genes regulated by miR-221 were evaluated using reverse-transcription polymerase chain reaction. Three types of cytomegalovirus (CMV)/Gluc_3' untranslated region (UTR) of homeobox B5 (HOXB5), which included a seed sequence of mature miR-221 in the 3' UTR of HOXB5 after the Gluc stop codon, were transfected into NPA cells, and pre-miR-221 was cotransfected with CMV/Gluc_3' UTR of HOXB5. The Gluc activities in cells were measured by luciferase assay. Mice implanted with PTC-expressing Gluc regulated by miR-221 were monitored with bioluminescence imaging for 6 d. **Results:** Microarray analysis showed thousands of genes were directly and indirectly regulated by miR-221 and shifted the gene expression pattern of normal thyroid cells toward PTC. Of several genes downregulated more than 2-fold by miR-221, messenger RNA levels of HOXB5 were significantly downregulated by miR-221. Also, in vitro or in vivo Gluc activities using CMV/Gluc_3' UTR of HOXB5 systems were downregulated dose dependently by endogenous or exogenous miR-221. **Conclusion:** MiR-221 overexpressed in PTC drives carcinoma gene expression patterns by directly and indirectly regulating numerous genes, including HOXB5. The bioluminescence imaging system using CMV/Gluc_3' UTR of HOXB5 is a useful tool for noninvasive in vivo long-term monitoring of functional targeting of miR-221.

Key Words: bioluminescence image; *Gaussia* luciferase; microarray; microRNA; papillary thyroid carcinoma

J Nucl Med 2008; 49:1686–1693
DOI: 10.2967/jnumed.108.052894

MicroRNAs (miRNAs) are small, noncoding RNAs that act as negative regulators of protein-coding gene expression (1,2). Mature miRNAs perfectly, or near perfectly, bind to complementary sequences in the 3' untranslated regions (UTRs) of target messenger RNAs (mRNAs) and cause either translational repression or mRNA degradation, depending on their degrees of complementarity or homology with target genes (3–6). Generally, miRNAs in animals are believed to cause translational repression due to partial pairing between miRNA and target mRNA. However, many reports have shown that transfected miRNAs can reduce the mRNA levels of their targets despite partial pairing (7–9). Microarray analysis to investigate changes in gene expression by transfection of miRNAs is a useful tool for studying the functional targeting of miRNAs (7).

Several reports have indicated that miRNAs play critical roles in essential biologic processes, including cellular differentiation, proliferation, apoptosis, and development (10–12). Also, deficiencies or excesses of miRNA functions in tissues have been correlated with several clinically important diseases, for example, cardiovascular, neurologic, and viral diseases; cancer; and metabolic disorders (11,13). In particular, miRNAs function as tumor suppressors or oncogenes because of aberrant expression, deletion, amplification, or mutation in human carcinogenesis (14–18). For instance, miRNA let-7 levels are depressed in lung cancer, as are those of miR-15a and miR-16-1 in B-cell chronic lymphocytic leukemia and miR-143 and miR-145 in colorectal cancer; miR-17-92 levels are elevated in lung cancer (19), and miR-18 and miR-224 are elevated in hepatocellular carcinoma. Moreover, miR-146b, miR-221, and miR-222 are upregulated in papillary thyroid carcinoma (PTC), which is the most common malignant thyroid tumor. In fact, it represents approximately 80% of all thyroid malignancies (20–25).

Even though the expression patterns of all known miRNAs have been compared in cancer and normal cells, the identification of miRNA target genes is a considerable challenge. Each miRNA can target hundreds of transcripts directly or indirectly, whereas more than 1 miRNA can converge on a single mRNA target. To date, several genes targeted by miRNAs have been identified. Examples

Received Mar. 25, 2008; revision accepted Jun. 9, 2008.
For correspondence or reprints contact: Soonhag Kim or June-Key Chung, Department of Nuclear Medicine, Seoul National University College of Medicine, 28 Yeongon-dong, Chongno-gu, Seoul, 110-744, Korea.
E-mail: kimsoonhag@empal.com; jkchung@plaza.snu.ac.kr
COPYRIGHT © 2008 by the Society of Nuclear Medicine, Inc.

include the targeting of Bcl₂ by miR-15a and miR-16-1, of RAS and MYC by let-7, of PTEN and RB2 by miR-17-92, of tropomyosin 1 by miR-21, and of KIT and p27^{kip1} by miR-221 and miR-222 (23,26,27). The variation in the expression level of each gene is caused by miRNAs, and this is highly prevalent in cancer because genomic aberration is closely associated with carcinogenesis. Therefore, searches for target genes of miRNAs influencing disease generation and investigations related to therapeutic uses of anti-miRNA are being actively pursued.

As the method to detect the molecular changes caused by miRNAs in vitro and in vivo, optical imaging using a bioluminescence reporter gene offers a noninvasive and repeated means of performing real-time analysis at the molecular level in living animals. Bioluminescence imaging involves the detection of light emitted by an enzymatic reaction and has low background luminescence levels. Of the bioluminescence reporter proteins firefly luciferase, *Renilla* luciferase, and *Gaussia* luciferase (Gluc), Gluc has the advantage that the emitted light is up to 1,000-fold more intense than that from native *Renilla* luciferase or firefly luciferase. Moreover, Gluc is the smallest luciferase known and is stable at elevated temperatures (28–30).

In this study, we transfected pre-miR-221 or anti-miR-221 into normal thyroid cells or PTC and performed microarray analysis to examine changes in the mRNA levels. Furthermore, we developed the Gluc imaging system for monitoring the gene targeted by miR-221 in vitro or in vivo and studied the effect of miR-221 on homeobox B5 (HOXB5), which is known to be directly regulated by miR-221, using a Gluc reporter system.

MATERIALS AND METHODS

Cell Lines and Culture Conditions

The human PTC cell line (NPA) was kindly provided by Dr. Do Joon Park (Department of Internal Medicine, Seoul National University College of Medicine), and the normal human thyroid cell line (HT-ori3) was kindly provided by Dr. Byung Il Kim

(Radiation Health Research Institute). HT-ori3 and NPA cells were maintained in RPMI 1640 supplemented with 100 units of penicillin per milliliter, 100 µg of streptomycin per milliliter, and 10% fetal bovine serum. All cells were incubated at 37°C in a 5% CO₂ humidified chamber.

Constructs and Transfection

Three types of the cytomegalovirus (CMV)/Gluc_{3'} untranslated region (UTR) of HOXB5, which included a seed sequence of mature miR-221 in the 3' UTR of HOXB5 after the Gluc stop codon, were constructed by annealing and subcloning the following oligonucleotides: CMV/Gluc_SR, containing 100-base pair (bp) oligonucleotides near the seed region (SR) that binds miR-221 in the 3' UTR of HOXB5; CMV/Gluc_{3xSR}, containing 3 repeats of the 34-bp SR that binds miR-221 in the 3' UTR of HOXB5; and CMV/Gluc_{MT}, containing completely changed sequences of the SR in the 3' UTR of HOXB5. The sequences of these oligonucleotides are shown in Table 1. Annealing was performed with a mixture of 200 pmol of oligonucleotides and 48 µL of annealing buffer containing 1× Tris–ethylenediaminetetraacetic acid buffer and 50 mM sodium chloride, using the following conditions: 95°C for 4 min and 70°C for 10 s, followed by slow cooling in a 70°C water bath for 90 min. The annealed oligonucleotide was subcloned into the XhoI and XbaI sites of CMV/Gluc vector (TargetingSystems).

The constructed plasmids were transfected into NPA cells. Briefly, cells were plated into 24-well plates the day before transfection at a seeding density of 1 × 10⁵ cells per well. Transfection was performed using Lipofectamine Plus reagent (Invitrogen), 0.3 µg of DNA, 4 µL of PLUS Reagent (Invitrogen), and 1 µL of Lipofectamine (Invitrogen) per well. Forty or 80 nM pre-miR-221 (Ambion) was cotransfected with 0.3 µg of CMV/Gluc_{3'} UTR of HOXB5; CMV/Gluc was used as an internal control to normalize the luciferase activities obtained from each experiment. All transfections were performed in quadruplicate.

Gluc Assay

Thirty hours after transfection, cells were washed with phosphate-buffered saline and treated with 100 µL of lysis solution. Supernatants were plated in microplates and Gluc activities were measured using a Wallac1420 VICTOR3V (PerkinElmer Life and

TABLE 1
Oligonucleotides Cloned in 3' UTR of Gluc

ID	Oligonucleotide sequence
SR of HOXB5 forward	5'- <u>tcgagt</u> gtctttgcccggcctgt CTCAGT GATTCGCTTTT GGTATTTGTTTGTAGCT ttctcgg-aagtcaaataa atgt-3'
SR of HOXB5 reverse	5'- <u>ctaga</u> catttatttgactccaggaa AGCTACAAACAAATACCAAAGCGAATCACTGAG ac-aggccccgcaa agacac-3'
3xSR of HOXB5 forward	5'- <u>tcgag</u> CTCAGT GATTCGCTTTT GGTATTTGTTTGTAGCT cat CTCAGT GATTCGCTTT TGGT ATTTGTTTGTAGCT cat CTCAGT GATTCGCTTTT GGTATTTGTTTGTAGCT t-3'
3xSR of HOXB5 reverse	5'- <u>ctaga</u> AGCTACAAACAAATACCAAAGCGAATCACTGAG atg AGCTACAAACAAATACCA AAAGCGAAT CACTGAG atg AGCTACAAACAAATACCAAAGCGAATCACTGA -Gc-3'
MT of HOXB5 forward	5'- <u>tcgag</u> AGTCAGG ATTCGCTTTT GGTATTTGTTTCACTACT cat AGTCAGG ATTCGCTTT TGGT ATTTGTTTCACTACT cat AGTCAGG ATTCGCTTTT GGTATTTGTTTCACTACT t-3'
MT of HOXB5 reverse	5'- <u>ctaga</u> AGTACTGA ACAAAT ACCAAAGCGAATCCTGACT atg AGTACTGA ACAAAT ACCA AAAGCGAAT CCTGACT atg AGTACTGA ACAAAT ACCAAAGCGAATCCTGACT c-3'

Underlined sequences indicate enzyme sites XhoI or XbaI. Bold sequences indicate binding sites of mature miR-221.

Analytic Sciences) using a luciferase assay kit (TargetingSystems). All data points are displayed as means \pm SDs ($n = 4$).

Total RNA Preparation and mRNA Microarray Analysis

HT-ori3 or NPA cells were plated into 10-cm dishes the day before transfection at a seeding density of 2×10^6 cells per dish. Pre-miR-221 (40 nM; Ambion) was then transfected into HT-ori3 cells, and anti-miR-221 (80 nM; Ambion) was transfected into NPA cells using Lipofectamine Plus (Invitrogen). At 0, 6, 24, and 48 h after transfection, cells were harvested. Total RNAs were isolated from HT-ori3 transfected with pre-miR-221 or NPA transfected with anti-miR-221 using Trizol reagent (Invitrogen), according to the manufacturer's instructions.

For control and test RNAs, the synthesis of target cRNA probes and hybridizations were performed using a Low RNA Input Linear Amplification Kit (Agilent Technologies). cRNA labeled with Cy3 was transcribed from dsDNA synthesized by reverse-transcription polymerase chain reaction (RT-PCR). Labeled cRNA was resuspended in $2\times$ hybridization buffer and directly pipetted onto an assembled human $4 \times 44K$ oligo microarray (Agilent Technologies).

Hybridization images were analyzed using GenePix Pro 6.0 (Axon Instruments). All data normalization and the selection of fold-changed genes were performed using GeneSpringGX 7.3 (Agilent Technologies). Intensity-dependent normalization (LOWESS) was performed, for which the ratio was reduced to the residual of the LOWESS fit of the intensity versus the ratio curve. Averages of normalized ratios were calculated by dividing the average of normalized signal channel intensities by the average of normalized control channel intensities.

RT-PCR Analysis of Target Genes Downregulated by miR-221

Total RNA was isolated from HT-ori3 cells or HT-ori3 cells treated with pre-miR-221 using Trizol reagent (Invitrogen). Total RNA was then reverse-transcribed in a final volume of 20 μ L containing 1 μ L of oligo (deoxythymidine), 4 μ L of 5_{first-strand} buffer, 2 μ L of 0.1 mol/L dithiothreitol, 1 μ L of 10 mmol/L deoxynucleotide triphosphate mix, and 50 units of Moloney murine leukemia virus reverse transcriptase (Invitrogen). The primers used for the different genes are shown in Table 2. RT-PCR of several genes targeted by miR-221 was then performed in a total volume of 20 μ L containing 100 ng of cDNA, 20 pmol of forward primer, 20 pmol of reverse primer, 5 μ L of 10 \times reaction buffer, 4 μ L of 10 mmol/L deoxynucleotide triphosphate mix, and 5 units of Taq-DNA polymerase using a GeneAmp PCR system (Applied Biosystems). Samples were then subjected to 5 min of denaturation at 94°C and 40 amplification cycles (60 s at 94°C, 30 s at each different temperature [shown in Table 2] followed by 60 s at

72°C), and followed by extension for 7 min at 72°C. β -actin was amplified over 25 cycles as a control using the same reaction solution. Amplified products were analyzed by ethidium bromide-stained agarose gel electrophoresis.

In Vivo Visualization of Gluc Expression in Cells

All experimental animals were housed under specific pathogen-free conditions and handled in accordance with the guidelines issued by the Institutional Animal Care and Use Committee of Seoul National University Hospital.

NPA cells were plated into 10-cm dishes the day before transfection at a seeding density of 2×10^6 cells per dish. To investigate the Gluc activities of CMV/Gluc_3xSR controlled by the binding of endogenous miR-221 to 3' UTR of HOXB5, 2×10^6 of NPA cells were suspended in 100 μ L of phosphate-buffered saline and implanted subcutaneously into 4 nude mice per group as follows: cells transfected with CMV/Gluc_MT into left thighs and cells transfected with CMV/Gluc_3xSR into right thighs. CMV/Gluc_MT as control was compared with CMV/Gluc. All mice were monitored for 6 d after implantation.

The IVIS100 imaging system (Xenogen), which includes an optical charge-coupled-device camera mounted on a light-tight specimen chamber, was used for the data acquisition and analysis. Briefly, coelenterazine (Biotium, Inc.) was diluted to 5 μ g/50 μ L in phosphate-buffered saline before use. Diluted coelenterazine (50 μ L) was subcutaneously injected into the sites of previous NPA cell injections. A mouse was placed in a specimen chamber with a mounted charge-coupled-device camera, and light emitted by luciferase in mice was then measured. Gray-scale photographic images and bioluminescent color images were superimposed using LIVINGIMAGE software (version 2.12; Xenogen) and IGOR image analysis software (WaveMetrics). Bioluminescence signals were expressed in units of photons per cubic centimeter per second per steradian.

RESULTS

Shift of Gene Expression Toward Pattern Shown in Cancer by miR-221 Overexpression

In vitro and in vivo luciferase assays demonstrated that mature miR-221 in PTC might function as oncogenes by downregulating various target genes by binding to SRs in the 3' UTR of target genes and by causing posttranscriptional regulation such as mRNA destabilization. We performed microarray analysis to follow the mRNA levels of the various genes up- or downregulated by miR-221.

TABLE 2
Primers Used for RT-PCR or Real-Time PCR

Genbank	Gene symbol	Forward primer	Reverse primer	Temperature
NM_001128	AP1G1	5' GCATTTAACACGGGGACCATCACAC 3'	5' TGCCAGCAATCACAACCTCCTT 3'	55°C
NM_001660	ARF4	5' CTAGGGCTTCAGTCTCTTCGTA 3'	5' GTTTAATATTCTGCCCAAACCA 3'	50°C
NM_194301	GARNL1	5' AAGCTGCGTCGTTCCCTCTGG 3'	5' AACTCCCCCTGCCCTCAA 3'	55°C
NM_002147	HOXB5	5' GGCGCATGAAGTGAAGAAGGACA 3'	5' GAGAGGGAGCCACAGGAAGACC 3'	52°C
NM_022566	MESDC1	5' GTGGTGTCCGGCCTGCGTCTC 3'	5' CTGGGGGTGAAGAAGGGTATGG 3'	55°C
NM_006451	PAIP1	5' GAGCGTAAGCGAAAACAGTA 3'	5' TGCAGCCAAAACAGTAGA 3'	52°C
NM_153020	RBM24	5' GCCAGTACCAGCCTCAGC 3'	5' TGTGCCCATTCCTCATTCTTAC 3'	56°C
NM_004171	SLC1A2	5' CGCATGAAGTGAAGAAGGAC 3'	5' GAGAGGGAGCCACAGGAAGACC 3'	55°C

On the basis of normalization and selection of fold-changed genes using GeneSpringGX7.3 (Agilent Technologies), 7,300 genes among 44,000 showed more than a 2-fold difference in mRNA level in at least 1 of 3 different time-course experiments of HT-ori3 cells exposed to exogenous pre-miR-221. Similarly, 5,778 genes were found to show more than a 2-fold difference in NPA exposed to anti-miR-221. To understand the effectiveness of miR-221 on carcinogenesis at the gene expression levels, we first compared genes showing 2-fold differences in NPA versus HT-ori3 cells and in pre-miR-221-treated HT-ori3 versus HT-ori3 cells. About 5,000 and 3,000 genes showed more than a 2-fold difference in gene expression in 2 of 3 different time-course experiments of NPA cells and pre-miR-221-treated HT-ori3 cells, respectively, compared with HT-ori3 cells. The ratios of overlapping genes (1,357 genes) identified by the 2 comparisons were converted to \log_{10} values and statistically evaluated using regression coefficients (R^2) (Fig. 1A). Even though the absolute ratios of many overlapping genes in these 2 comparisons showed relatively large differences, 92% of 1,357 genes showed a positive correlation pattern between mRNA levels in HT-ori3-treated pre-miR-221 and mRNA levels in NPA. Twenty-two percent of the 1,357 genes were upregulated and 70% were downregulated by more than 2-fold, compared with mRNA levels in HT-ori3. The R^2 value of the 1,357 genes between the 2 comparisons was 0.552.

Second, we compared the genes upregulated by treatment with pre-miR-221 in HT-ori3 (a normal thyroid [NT] cell line) or downregulated by anti-miR-221 in NPA cells (a

PTC cell line) with genes related to thyroid neoplasms, using information available at <http://www.sabiosciences.com>. The analyzed genes were classified by 53 of upregulated genes in HT-ori3 treated with pre-miR-221 and 65 of downregulated genes in NPA treated with anti-miR-221, respectively (data are available as Supplemental Tables 1 and 2; supplemental materials are available online only at <http://jnm.snmjournals.org>).

In particular, the 9 genes cyclin D2 (CCND2); heat shock 70-kDa protein 4 (HSPA4); Pinin, desmosome-associated protein (PNN); kinesin family member 3B (KIF3B); signal transducer and activator of transcription 2 (STAT2); chromatin assembly factor 1, subunit A (p150) (CHAF1A); x-ray repair complementing defective repair in Chinese hamster cells 1 (XRCC1); TSPY-like 2 (TSPYL2); and DEAD (Asp-Glu-Ala-Asp) box polypeptide 54 (DDX54) were upregulated in HT-ori3 treated with pre-miR-221 and downregulated in NPA treated with anti-miR-221.

Genes Regulated by miR-221

To search for genes directly targeted by miR-221, 3,800 genes downregulated by more than 2-fold in HT-ori3 cells treated with pre-miR-221 and 1,900 genes downregulated by 2-fold or more in NPA treated with anti-miR-221 were analyzed using the 279 target genes of miR-221 predicted by PicTar DB (available at <http://pictar.bio.nyu.edu>), which is one of the algorithms commonly used to identify human miRNA gene targets. A total of 19 genes downregulated in pre-miR-221-treated HT-ori3 and 13 genes upregulated in anti-miR-221-treated NPA were classified by comparing

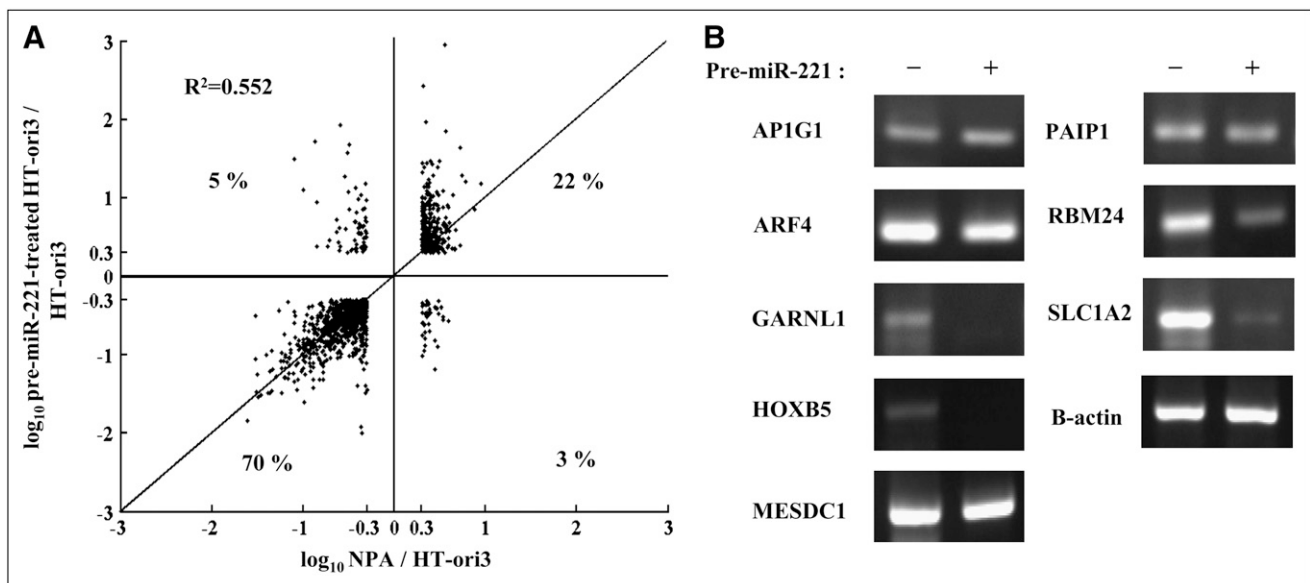


FIGURE 1. Variation of gene expression by miR-221 in thyroid cells. (A) Correlation between gene patterns regulated by miR-221 overexpressed in NT cells and gene pattern in PTC cells. Fold expressional differences of 1,357 genes that exhibited more than 2-fold differences in NPA vs. HT-ori3 (x-axis) and in HT-ori3 treated with pre-miR-221 vs. HT-ori3 (y-axis) were drawn on scatter plots. All values are expressed as \log_{10} of fold expressional differences. R^2 of 1,357 genes = 0.552. (B) Comparisons of RNA levels of miR-221 target gene candidates, AP1G1, ARF4, GARNL1, HOXB5, MESDC1, PAIP1, RBM24, and SLC1A2, in HT-ori3 and pre-miR-221-treated HT-ori3 cells. mRNA levels of each gene were determined by propagating from cDNA synthesized with total RNA obtained from HT-ori3 or 80 nM of pre-miR-221-treated HT-ori3 cells.

them with PicTar DB–predicted target gene candidates (Supplemental Tables 3 and 4). Of these 19 target gene candidates, Adaptor-related protein complex 1, γ -1 subunit (APIG1), ADP-ribosylation factor 4 (ARF4), GTPase activating Rap/Ran GAP domainlike 1 (GARNL1), homeobox B5 (HOXB5), mesoderm development candidate 1 (MESDC1), poly(A) binding protein interacting protein 1 (PAIP1), RNA binding motif protein 24 (RBM24), and solute carrier family 1 (glial high-affinity glutamate transporter), member 2 (SLC1A2) genes were randomly selected and compared with their mRNA levels in HT-ori3 and pre-miR-221–treated HT-ori3 using RT-PCR. The mRNA levels of the selected genes were found to be significantly downregulated in HT-ori3 cells treated with exogenous pre-miR-221 as compared with untreated HT-ori3 cells (Fig. 1B).

HOXB5 Regulation of miR-221

The HOXB5 gene was dramatically downregulated by exogenous pre-miR-221 in HT-ori3 cells and shows a tendency to be repressed in several cancers (31–33). Thus, it was chosen for further study as a potential miR-221 target using our *in vitro* or *in vivo* bioluminescent reporter system. The miR-221 SR in the 3' UTR of HOXB5 was searched for in PicTar DB and cloned into CMV/Gluc reporter vector (Fig. 2A). To acquire comparable imaging signals from the miR-221-regulated HOXB5 gene in carcinoma, 2 different types of nucleotides containing single or triple copies of the miR-221 SR of HOXB5 were designed as follows: 100 bp from the 3' UTR of HOXB5 near the SR (designated CMV/Gluc_SR) and 3 copies of the 34-bp nucleotide-binding mature miR-221 (designated CMV/Gluc_3xSR). Gluc activities of NPA cells transfected with CMV/Gluc_SR or CMV/Gluc_3xSR were slightly decreased by endogenous miR-221. Also, *in vitro* luciferase assays in NPA cells treated with exogenous pre-miR-221 showed that the Gluc activities of CMV/Gluc_SR and CMV/Gluc_3xSR were significantly and gradually decreased as pre-miR-221 doses were increased versus reporter genes containing a mutant sequence of the SR, CMV/Gluc_MT construct (Fig. 2B). All Gluc activities from 3 different constructs treated with 0, 40, and 80 nM pre-miR-221 were normalized by Gluc intensity of CMV/Gluc. Interestingly, Gluc activity of CMV/Gluc_3xSR regulated by pre-miR-221 had a higher repressive effect than did CMV/Gluc_SR. This finding was due to the better bioluminescent signal contrast obtained from the CMV/Gluc_3xSR construct when monitoring the repression of miR-221-targeted HOXB5, as compared with that obtained from the CMV/Gluc_SR construct, which contained only a single copy of the miR-221 SR.

For the *in vivo* real-time monitoring of endogenous miR-221 targets in PTC, NPA cells transfected with a set of CMV/Gluc and CMV/Gluc_MT (Fig. 3A) or CMV/Gluc_MT and CMV/Gluc_3xSR (Fig. 3B) were implanted into nude mice. Gluc activities, which represented the endogenous regulation of HOXB5 by mature miR-221, were monitored for 6 d and subjected to region-of-interest

(ROI) analysis (Fig. 3B). For monitoring of the CMV/Gluc_MT construct, CMV/Gluc as an internal control was detected and compared. The Gluc expression of CMV/Gluc and CMV/Gluc_MT was reduced at a similar rate over time, because of transient transfection of the reporter vectors into NPA cells (Fig. 3A). Compared with controls (CMV/Gluc_MT), Gluc expression of CMV/Gluc_3xSR significantly and gradually was reduced over the 6-d observation period and was barely detectable on the final day, whereas Gluc expression of CMV/Gluc_MT was decreased over time, though at a slower rate than CMV/Gluc_3xSR (Fig. 3B). Gluc repression of CMV/Gluc_3xSR indicated that mature miR-221 is highly expressed and suggests that HOXB5 is directly regulated by mature miR-221 in PTC. Although the ROI of CMV/Gluc_3xSR for 2 d after implantation was similar to that of CMV/Gluc_MT, ROI analysis on days 3 and 6 showed that it had reduced 1.8- and 2.8-fold, respectively, versus that of CMV/Gluc_MT (Fig. 3B).

DISCUSSION

MicroRNAs play critical roles in cellular differentiation, proliferation, apoptosis, and development and correlated with clinically important diseases, such as cancer; cardiovascular, neurologic, and viral diseases; and metabolic disorders (11,13). The abnormalities of specific miRNA expression contribute to the initiation and progression of tumors (14–18). Of the many miRNAs known, miR-146b, miR-221, and miR-222 have recently been reported to be highly expressed in PTC (20–25). In our preliminary study of miRNA expression in PTC cell lines (TPC-1 and NPA), real-time PCR showed that the expression of miR-221 in NPA and TPC-1 cells, respectively, was 17 and 7 times more than that in HT-ori3 cells, whereas the expression of miR-146b and miR-222 was slightly overexpressed in PTC cells (data not shown). On the basis of these results, miR-221 was selected for this study. MiR-221 is intergenic miRNA located on chromosome Xp11.3, in which it clusters with miR-222. Moreover, the sequence of mature miR-221 is evolutionarily well conserved from worm to man (22,23).

An miRNA targets several thousands of mRNAs that related to oncogenic or antioncogenic genes. In the present study, we found a significant correlation between miR-221 and the regulation of gene expression using RT-PCR and a microarray approach and noninvasively monitored the functional targeting of miR-221 in living animals using our luciferase reporter system.

Generally, miRNAs are known to bind to the 3' UTR of their targets and thereby to cause mRNA degradation or translational inhibition. Unlike other single tissue-specific or disease-specific eukaryotic genes, microarray analysis and PicTar DB demonstrated that miRNAs directly target hundreds or even thousands of coding mRNAs (7,34,35). The overexpression of several tissue-specific miRNAs,

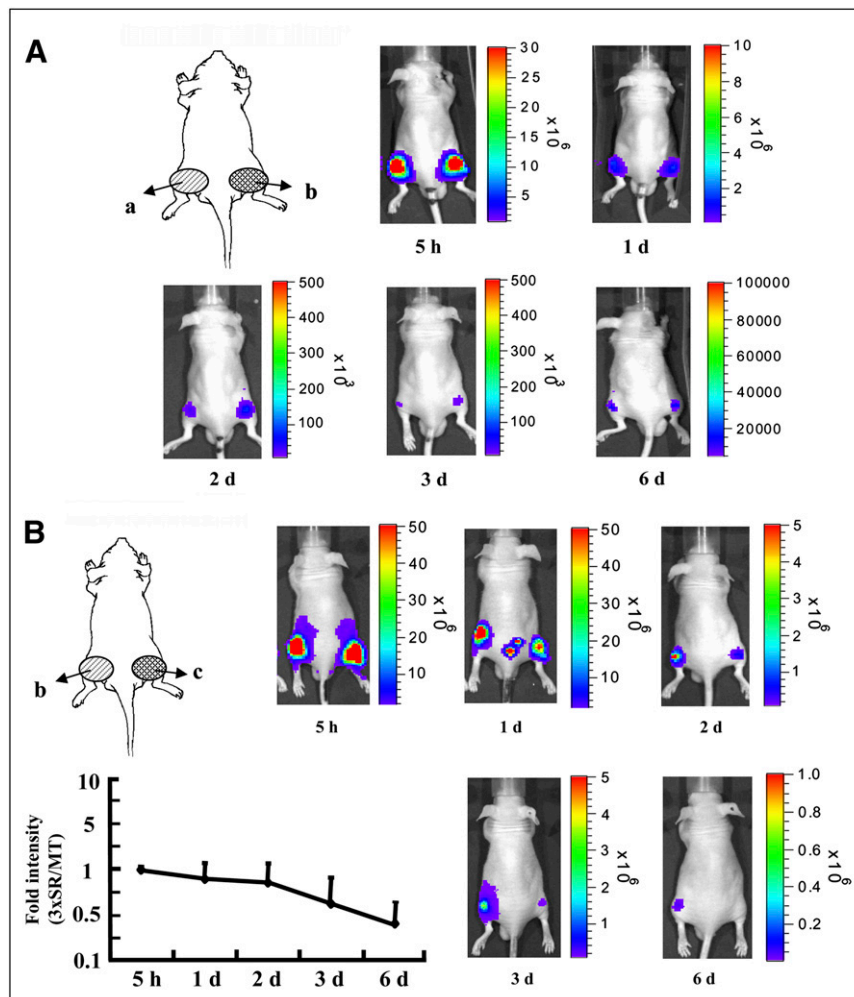


FIGURE 3. Real-time monitoring of Gluc activities controlled by binding of miR-221 to 3' UTR of HOXB5 in nude mice implanted with NPA cells. Images were obtained at 5 h and at 1, 2, 3, and 6 d after implanting NPA cells subcutaneously into nude mice. (A) Comparison of Gluc activities of CMV/Gluc and CMV/Gluc_MT. (B) Gluc activities repressed by binding of endogenous miR-221 to CMV/Gluc_3xSR and fold ratio from ROI analysis of CMV/Gluc_MT in left thigh and CMV/Gluc_SR in right thigh for 6 d. All data were normalized vs. ROIs of cells transfected with CMV/Gluc_MT. ROI data are displayed as means \pm SD (fold intensity; $n = 4$ mice/group). a = cells transfected with CMV/Gluc; b = cells transfected with CMV/Gluc_MT; c = cells transfected with CMV/Gluc_3xSR.

or anti-miRNAs that regulate target genes related to cancer development could be used to treat thyroid carcinoma warrants attention. However, for the therapeutic application of miRNAs overexpressed in cancers, the stability and intracellular delivery of pre-miRNAs or anti-miRNAs in the living organism first needs to be solved. Our single-reporter-gene system, developed to monitor endogenous miRNA targets, or the ongoing development of a simultaneous dual-luciferase imaging system for miR-221 based on firefly luciferase and for target genes based on Gluc, will provide more noninvasive information about the biogenesis and function of other miRNAs involved in carcinogenesis development for effective cancer therapies and cancer pharmacokinetics.

CONCLUSION

The present study demonstrated that miR-221, which is overexpressed in PTC, functions as an oncogene through the posttranscriptional regulation of many genes directly or indirectly and through the ability of the luciferase system to functionally target miR-221 in PTC. Further work should be done to identify genes targeted by miR-221 in cancer tissues other than PTC. The finding of other target genes

that are crucial to oncogenesis or antioncogenesis could provide the possibility for cancer treatment using pre-miRNAs or anti-miRNAs.

ACKNOWLEDGMENTS

This work was funded by Korean Science and Engineering Foundation (KOSEF) grant 2007-02242 from the Korean government (MOST), by the Seoul R&BD program, by the National R&D Program for Cancer Control of Ministry of Health & Welfare (0820320), and by the BK21 Project for Medicine, Dentistry, and Pharmacy in Korea (2007).

REFERENCES

1. Bartel DP. MicroRNAs: genomics, biogenesis, mechanism, and function. *Cell*. 2004;116:281–297.
2. Ambros V. The functions of animal microRNAs. *Nature*. 2004;431:350–355.
3. Zeng Y, Yi R, Cullen BR. MicroRNAs and small interfering RNAs can inhibit mRNA expression by similar mechanisms. *Proc Natl Acad Sci USA*. 2003;100:9779–9784.
4. Bagga S, Bracht J, Hunter S, et al. Regulation by let-7 and lin-4 miRNAs results in target mRNA degradation. *Cell*. 2005;122:553–563.
5. Wu L, Fan J, Belasco JG. MicroRNAs direct rapid deadenylation of mRNA. *Proc Natl Acad Sci USA*. 2006;103:4034–4039.
6. Valencia-Sanchez MA, Liu J, Hannon GJ, Parker R. Control of translation and mRNA degradation by miRNAs and siRNAs. *Genes Dev*. 2006;20:515–524.

7. Lim LP, Lau NC, Garrett-Engle P, et al. Microarray analysis shows that some microRNAs downregulate large numbers of target mRNAs. *Nature*. 2005; 433:769–773.
8. Hurteau GJ, Spivack SD, Brock GJ. Potential mRNA degradation targets of hsa-miR-200c, identified using informatics and qRT-PCR. *Cell Cycle*. 2006; 5:1951–1956.
9. Hurteau GJ, Carlson JA, Spivack SD, Brock GJ. Overexpression of the microRNA hsa-miR-200c leads to reduced expression of transcription factor 8 and increased expression of E-cadherin. *Cancer Res*. 2007;67:7972–7976.
10. Brennecke J, Hipfner DR, Stark A, Russell RB, Cohen SM. bantam encodes a developmentally regulated microRNA that controls cell proliferation and regulates the proapoptotic gene hid in *Drosophila*. *Cell*. 2003;113:25–36.
11. Kloosterman WP, Plasterk RH. The diverse functions of microRNAs in animal development and disease. *Dev Cell*. 2006;11:441–450.
12. Jovanovic M, Hengartner MO. miRNAs and apoptosis: RNAs to die for. *Oncogene*. 2006;25:6176–6187.
13. Weiler J, Hunziker J, Hall J. Anti-miRNA oligonucleotides (AMOs): ammunition to target miRNAs implicated in human disease? *Gene Ther*. 2006;13:496–502.
14. Osada H, Takahashi T. MicroRNAs in biological processes and carcinogenesis. *Carcinogenesis*. 2007;28:2–12.
15. Lu J, Getz G, Miska EA, et al. MicroRNA expression profiles classify human cancers. *Nature*. 2005;435:834–838.
16. Zhang B, Pan X, Cobb GP, Anderson TA. microRNAs as oncogenes and tumor suppressors. *Dev Biol*. 2007;302:1–12.
17. Esquela-Kerscher A, Slack FJ. Oncomirs: microRNAs with a role in cancer. *Nat Rev Cancer*. 2006;6:259–269.
18. Calin GA, Croce CM. MicroRNA signatures in human cancers. *Nat Rev Cancer*. 2006;6:857–866.
19. Akao Y, Nakagawa Y, Naoe T. MicroRNA-143 and -145 in colon cancer. *DNA Cell Biol*. 2007;26:311–320.
20. Nikiforova MN, Tseng GC, Steward D, Diorio D, Nikiforov YE. MicroRNA expression profiling of thyroid tumors: biological significance and diagnostic utility. *J Clin Endocrinol Metab*. 2008;93:1600–1608.
21. Gillies JK, Lorimer IA. Regulation of p27Kip1 by miRNA 221/222 in glioblastoma. *Cell Cycle*. 2007;6:2005–2009.
22. Pallante P, Visone R, Ferracin M, et al. MicroRNA deregulation in human thyroid papillary carcinomas. *Endocr Relat Cancer*. 2006;13:497–508.
23. Felli N, Fontana L, Pelosi E, et al. MicroRNAs 221 and 222 inhibit normal erythropoiesis and erythroleukemic cell growth via kit receptor down-modulation. *Proc Natl Acad Sci USA*. 2005;102:18081–18086.
24. He H, Jazdzewski K, Li W, et al. The role of microRNA genes in papillary thyroid carcinoma. *Proc Natl Acad Sci USA*. 2005;102:19075–19080.
25. Visone R, Russo L, Pallante P, et al. MicroRNAs (miR)-221 and miR-222, both overexpressed in human thyroid papillary carcinomas, regulate p27Kip1 protein levels and cell cycle. *Endocr Relat Cancer*. 2007;14:791–798.
26. Galardi S, Mercatelli N, Giorda E, et al. miR-221 and miR-222 expression affects the proliferation potential of human prostate carcinoma cell lines by targeting p27Kip1. *J Biol Chem*. 2007;282:23716–23724.
27. le Sage C, Nagel R, Egan DA, et al. Regulation of the p27^{Kip1} tumor suppressor by miR-221 and miR-222 promotes cancer cell proliferation. *EMBO J*. 2007; 26:3699–3708.
28. Ottobriani L, Ciana P, Biserni A, Lucignani G, Maggi A. Molecular imaging: a new way to study molecular processes in vivo. *Mol Cell Endocrinol*. 2006; 246:69–75.
29. Tannous BA, Kim DE, Fernandez JL, Weissleder R, Breakefield XO. Codon-optimized Gaussia luciferase cDNA for mammalian gene expression in culture and in vivo. *Mol Ther*. 2005;11:435–443.
30. Doubrovin M, Serganova I, Mayer-Kuckuk P, Ponomarev V, Blasberg RG. Multimodality in vivo molecular-genetic imaging. *Bioconjug Chem*. 2004;15:1376–1388.
31. Calin GA, Sevignani C, Dumitru CD, et al. Human microRNA genes are frequently located at fragile sites and genomic regions involved in cancers. *Proc Natl Acad Sci USA*. 2004;101:2999–3004.
32. Cillo C, Faiella A, Cantile M, Boncinelli E. Homeobox genes and cancer. *Exp Cell Res*. 1999;248:1–9.
33. Lopez R, Garrido E, Pina P, et al. HOXB homeobox gene expression in cervical carcinoma. *Int J Gynecol Cancer*. 2006;16:329–335.
34. Grün D, Wang Y-L, Langenberger D, Gunsalus KC, Rajewsky N. microRNA target predictions across seven *Drosophila* species and comparison to mammalian targets. *PLoS Comput Biol*. 2005;1:e13.
35. Krek A, Grun D, Poy MN, et al. Combinatorial microRNA target predictions. *Nat Genet*. 2005;37:495–500.
36. Yekta S, Shih IH, Bartel DP. MicroRNA-directed cleavage of HOXB8 mRNA. *Science*. 2004;304:594–596.
37. Cillo C, Barba P, Freschi G, Bucciarelli G, Magli MC, Boncinelli E. HOX gene expression in normal and neoplastic human kidney. *Int J Cancer*. 1992; 51:892–897.